Electronics and Electrical Engineering

https://www.aimspress.com/journal/ElectrEng

AIMS Electronics and Electrical Engineering, 10(2): 180–204.
DOI: 10.3934/electreng.2026008
Received: 16 October 2025
Revised: 08 January 2026
Accepted: 26 January 2026
Published: 02 March 2026

Research article

Planning strategies for distributed photovoltaic based on fuzzy cognitive maps

Jiancheng Sha[1], Shaojun Bian[2], Lingfang Sun[1], Mengchao Xu[3] and Guoliang Feng[1,*]

[1] School of Automation Engineering, Northeast Electric Power University, Jilin City, China
[2] School of Creative and Digital Industries, Buckinghamshire New University, High Wycombe HP11 2JZ, UK
[3] School of Control and Computer Engineering, North China Electric Power University, Beijing, China

* **Correspondence:** Email: fengguoliang@neepu.edu.cn; Tel: +8613614427850.

Abstract: With the increasing penetration of distributed photovoltaic (PV) generation in distribution grids, PV access locations significantly affect voltage stability and network losses. In this paper, we proposed a critical node identification and PV access planning method based on fuzzy cognitive maps (FCMs). An FCM-based distribution grid model was established by incorporating time-varying load characteristics and PV output fluctuations, and the weight matrix was learned from historical operating data using a data-driven optimization approach. A node importance index derived from out-degree centrality was then proposed to identify critical nodes in the distribution grid. Simulation studies on the IEEE 33-node and 118-node standard test systems under different PV penetration levels demonstrated that connecting PV to non-critical nodes effectively mitigates voltage fluctuations and reduces system power losses compared with critical-node-based access strategies. The proposed method provides an interpretable and effective decision-support tool for distributed PV integration in distribution grids.

Keywords: fuzzy cognitive maps; intelligent computing; distribution grid; photovoltaic; energy loss

1. Introduction

With the rapid development of distributed photovoltaic (PV) generation, an increasing number of PV systems are being integrated into distribution grids. While distributed PV and other forms of distributed generation can effectively promote renewable energy utilization, reduce fossil fuel consumption, and improve energy efficiency by supplying power close to loads, their access locations have a significant impact on distribution grid operation. Inappropriate PV connection points may lead to voltage fluctuations, increased power losses, harmonic issues, and voltage limit violations, especially

under time-varying load demand and PV output conditions [1]. Moreover, distribution system operators often have limited controllability over PV access locations, which further exacerbates these operational challenges. Therefore, identifying suitable access locations for distributed PV has become a critical issue in distribution grid planning and operation. This problem essentially depends on accurately identifying the critical nodes within the distribution grid that exert a dominant influence on system performance, which remains challenging due to the coupled effects of grid topology and dynamic operating states [2].

There are three major research methodologies on crucial node identification methods for distribution grid that are available: (1) The key nodes are identified based on the network architecture, and their criticality is determined by their positional information and transmission role in the network, which is based on complex network theory. This approach typically investigates only the distribution grid's structural vulnerability and overlooks the influence of network features; hence, the operational condition of the network cannot be studied using this approach. Liu et al. [3] proposed node electrical centrality, distribution grid vulnerability indicators, and networkability indicators based on the theory of complex network centrality to analyze the transmission capacity and performance of distribution grid during operation. Zhu et al. [4] employed an improved PageRank algorithm to identify critical nodes by combining distribution grid topology and different types of nodes, and the distribution grid was segmented based on the identification results to prevent cascading faults in the power system. (2) The key nodes in the grid are recognized by their operational status, and their relevance is determined using the grid's real operational parameters, with trend calculation serving as the foundation. Zhang et al. [5] presented a new risk index based on risk theory to measure the risk of power lines in power systems by taking the order of likelihood and severity of accidents into account. Yang et al. [6] established a new energy grid to obtain fundamental fault identification parameters, weak area identification parameters, and a line weak indicator model to identify the weak areas in the new energy grid. (3) The significance of nodes was determined by a combination of topology and operational status. The researchers in [7] employed node resilience, node voltage deviation, and line loss changes as identifiers, and considered the system's safety and economy, as well as the time of the load and PV outputs. Wang et al. [8] introduced the idea of the "link strength" of distribution grid nodes based on a trend-tracking method that computes node relevance in terms of global topology. Liu et al. [9] developed key node identification indices based on the three aspects of node security, importance, and controllable potential, as well as the time-varying characteristics of the distribution grid system, and dynamically identified and analyzed the distribution grid with distributed power output.

Although critical node identification methods have achieved certain success in distribution grid analysis, their applicability to distributed photovoltaic access planning remains limited. Topology-based methods primarily focus on network structural characteristics and are generally independent of operating conditions, making them insufficient for capturing the dynamic impacts of time-varying loads and PV outputs. Operation-state-based methods rely heavily on real-time measurements or scenario-based simulations, which can reflect system operating conditions but often lack interpretability and generalization capability. Hybrid methods attempt to combine topology and operational information; however, they are usually designed for static or quasi-static scenarios and struggle to represent complex causal relationships among nodes under continuously changing operating states.

In contrast, fuzzy cognitive maps provide a unified framework that naturally integrates network topology, operating states, and causal relationships among system variables. By representing

distribution grid nodes as concepts and their interactions as weighted causal links, FCMs are well suited for modeling complex, nonlinear, and time-varying systems. The learned weight matrix further offers semantic interpretability, enabling quantitative assessment of node influence and facilitating critical node identification under dynamic operating conditions. Compared with topology-based, operation-state-based, and hybrid methods, FCM-based approaches can simultaneously capture the coupled effects of grid topology and temporal variations in load demand and PV output, which are essential for distributed PV access planning problems. To further clarify the differences among critical node identification methods and highlight the suitability of fuzzy cognitive maps for the problem considered in this paper, a comparative summary of representative approaches is provided in Table 1. It should be noted that fuzzy cognitive maps are not the only possible approach for critical node identification in distribution grids, and alternative methods may provide useful insights under assumptions and application scenarios. However, given our objectives of this study, namely identifying critical nodes for distributed photovoltaic access under time-varying operating conditions while maintaining interpretability, fuzzy cognitive maps offer a particularly suitable modeling framework, as their characteristics are well aligned with the problem formulation considered in this paper.

Table 1. Comparison of critical node identification methods for distribution grids.

Method category	Main characteristics	Time-varying capability	Limitations	References
Topology based	Network structure and graph metrics.	Low	Ignore operating states and PV variability	[3, 4]
Operation state based	Real time or scenario based parameters.	Moderate	High data dependence; limited generalization	[5, 6]
Hybrid	Combine topological and operational indicators.	Moderate	Often static or quasi-static; complex modeling	[7–9]
FCM based (this paper)	Integrates topology, operating states, and causal relationships.	High	Requires historical data for training	-

A fuzzy cognitive maps is a knowledge representation with a graph network structure, consisting of nodes and connections, where nodes represent concepts or variables and links reflect interactions between them. FCMs can be used as a mathematical modeling technique for representing and analyzing complex nonlinear systems, especially in the field of artificial intelligence and decision-making. In recent years, FCMs have been widely used in the fields of describing complex dynamical systems [10–12], forecasting and modeling of time series [13–15], systematic risk assessment and management [16–18], and pattern recognition [19–21].

Fuzzy cognitive maps exhibit multiple advantages in handling complex systems and uncertainty issues due to their unique characteristics [22, 23]:

1. FCMs visually present the causal relationships between concepts through nodes and weighted directed edges, making the understanding and analysis of complex systems easier.

2. The structure of FCMs enables users to adjust and update the model in a timely manner based on new information or changing conditions, thereby enhancing the model's adaptability and flexibility.
3. FCMs can be used for systems analysis, aiding in the identification of key factors and potential areas for improvement, as well as considering causal relationships in system design.
4. Unlike the black-box models of neural networks, FCMs possess semantic interpretability. They enable understanding and interpreting the information and data processing procedures within the map through the nodes and connections.
5. FCMs can be combined with analytical methods, such as sensitivity analysis, path analysis, and network analysis, to provide a more comprehensive understanding of the system.

Fuzzy cognitive maps differ from neural network black-box models in that they have semantic interpretability, which can be used to understand and interpret the information in the FCMs, the data processing process through the nodes, and connections, where the connections between the nodes can explain how the nodes interact with each other. Based on the foregoing characteristics, it is assumed that the distribution grid nodes correspond to the conceptual nodes in the FCMs so that the values in the learned weight matrix indicate the mutual influence relationship between the nodes, and the degree of influence between the nodes can be further analyzed to find the distribution grid's critical nodes. This also provides non-critical nodes that can be linked to the distributed PV.

Distribution grids are time-varying, their state and performance change over time, and the demand for electricity by customers changes over time. Moreover, load size and characteristics can fluctuate over time, causing changes in distribution grid factors such as current and voltage. Furthermore, the use of renewable energy can cause oscillations in power generation in the distribution grid, altering the distribution grid's power supply and load balance. Moreover, FCMs can be used to model time series, build input nodes and connections for FCMs, and incorporate the time dimension to account for system dynamics in order to reflect the system's state and features at different points in time. This combination improves the ability of FCMs to deal with dynamic systems and time-series data, improving the modeling and solving of time-varying problems.

In summary, we apply fuzzy cognitive maps to critical node identification in distribution grids, enabling informed PV access decisions that improve voltage stability and reduce power losses in practical grid planning and operation while offering a transparent and data-driven framework for distribution grid analysis under dynamic and uncertain conditions.

The following are the major contributions of the suggested method:

(1) Using FCMs to examine the extent to which each node in the network affects network performance, and model a distribution grid with dynamic loads and dynamic PV outputs.
(2) The node importance index is proposed to select the key nodes of the distribution grid containing distributed power sources based on the weight matrix of the fuzzy cognitive maps, and the time-varying nature of the distribution grid loads and PV outputs is taken into account when considering the distribution grid topology, which further strengthens the accuracy of the identification of the key nodes.
(3) Although FCMs have been applied in power and energy decision-support problems, their use for data-driven critical node identification and PV access planning in distribution grids under time-varying operating conditions remains limited [24–26]. In this study, we develop an

interpretable FCM-based framework that integrates network topology with temporal operating data to evaluate node importance and support PV access decisions.

The remainder of the paper is structured as follows: in Section 2, we delve into the fundamental notions of the FCMs. In Section 3, we describe the FCMs modeling methodology and recommend node importance to identify essential nodes in a distribution grid. In Section 4, we describe the experiments and compare the outcomes. In Section 5, we provide the conclusion.

2. Fuzzy cognitive maps

Fuzzy cognitive maps is a soft computing method that combines fuzzy logic and neural networks proposed by Kosko [27]. The topology of fuzzy cognitive maps can be represented as a weighted directed graph with a feedback mechanism composed of concept nodes, arcs, and weights. Figure 1 depicts a simplified FCMs with five conceptual nodes. Conceptual nodes are the basic units of fuzzy cognitive maps and can represent specific events, values, goals, etc., so that the nodes have a precise meaning in the system under study. In fuzzy cognitive maps, the relationships between nodes are represented by directed edges, and the effective connections between nodes represent logical relationships between conceptual nodes. The above features make fuzzy cognitive maps simple and intuitive to represent.

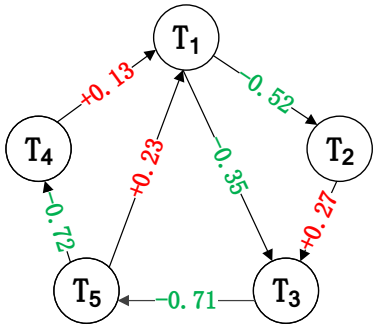

$$W = \begin{bmatrix} 0 & -0.52 & -0.35 & 0 & 0 \\ 0 & 0 & +0.27 & 0 & 0 \\ 0 & 0 & 0 & 0 & -0.71 \\ +0.13 & 0 & 0 & 0 & 0 \\ +0.23 & 0 & 0 & -0.72 & 0 \end{bmatrix}$$

Figure 1. The structure and the weight matrix of a 5-node FCM.

The semantics of a FCM containing individual nodes can be represented by a 4-tuple $U = (C, W, A, f)$, where $C = \{C_1, C_2, \ldots, C_n\}$ is the set of nodes of the FCMs , and W is a $n \times n$ dimensional weight matrix:

$$\boldsymbol{W} = \begin{bmatrix} w_{11} & w_{12} & \cdots & w_{1n} \\ w_{21} & w_{22} & \cdots & w_{2n} \\ \vdots & \vdots & \vdots & \vdots \\ w_{n1} & w_{n2} & \cdots & w_{nn} \end{bmatrix} = [\boldsymbol{W}_1, \boldsymbol{W}_2, ..., \boldsymbol{W}_n]$$

where $w_{ij} \in [-1\ ,\ 1]$, $i, j = 1, 2, \ldots, n$, expresses the strength of the causal influence between the cause and effect nodes, and n is the number of nodes. $w_{ij} > 0$ indicates that nodes C_i and C_j are positively causal related. $w_{ij} = 0$ indicates that nodes C_i and C_j have no causal relationship, and $w_{ij} < 0$ indicates that nodes C_i and C_j are negatively causal related. $A_i(t)$ is the state of the node C at time t. The node state A at time $t + 1$ can be described as:

$$A_j(t+1) = f(\sum_{i=1}^{N} \boldsymbol{A}_i(t) w_{ij}) \tag{2.1}$$

where $f(\bullet)$ is an activation function that can restrict the expression value of a node to a unit range. The commonly used activation functions in FCMs include the following:

(1) The bivalent function.

$$f(x) = \begin{cases} 1, x > 0 \\ 0, x \leq 0 \end{cases} \tag{2.2}$$

(2) The trivalent function.

$$f(x) = \begin{cases} -1, x < 0 \\ 0, x = 0 \\ 1, x > 0 \end{cases} \tag{2.3}$$

(3) The sigmoid function.

$$f(x) = \frac{1}{1 + e^{-\lambda x}} \tag{2.4}$$

According to the literature [28, 29], the use of bivalent function or trivalent function in fuzzy cognitive maps does not effectively represent changes in the state values of concepts. Although they can always converge to a fixed-point attractor or limit cycle, the number of their distinct states is limited. On the other hand, the sigmoid function offers higher precision in representing the activation values of concepts, providing a greater advantage in building precise models. In Eq. (4) , parameter $\lambda > 0$ can determine the slope of the activation function at the origin. The value of λ is chosen by the nature of the different systems, and small values of λ are more suitable for highly nonlinear systems. According to the literature [30, 31], when selecting the sigmoid function as the activation function, it is necessary to consider the convergence of the fuzzy cognitive map model. To determine whether a FCM converges, the model can be subjected to a large number of discrete time steps T, after which its mapping states can be observed for judgment. Any FCMs will inevitably reach one of three states: A fixed point, a limit cycle, or a chaotic state. Research suggests that the value of λ is usually set to 5 [32], and we have verified the convergence of the FCM model in this paper. The model converges to a fixed point.

3. Methodology

An FCMs-based approach for finding the location of PV access in the distribution grid is suggested to determine the distribution of critical nodes in the distribution grid system. We assess the significance of distribution grid nodes using the interpretability of fuzzy cognitive maps. The approach is based on hourly distribution grid load data and calculates system currents at the relevant moments, taking into account the load distribution and the variability of the PV output. The load flow calculation findings are utilized to model the distribution system, learn the relevant weight matrix, and establish the access strategy for distributed PV generation based on the weight matrix's distribution of conceptual weights.

3.1. FCMs modeling of distributed grids

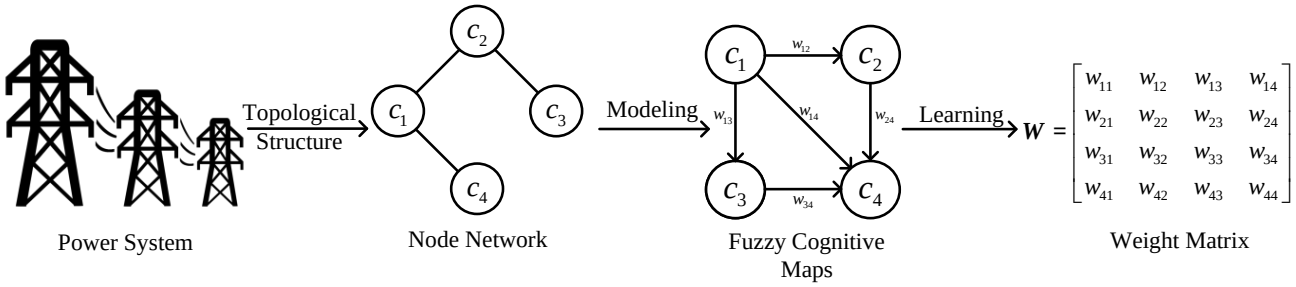

Figure 2. Modeling process of a distribution grid based on FCMs.

For FCMs, the purpose of weight learning is to find an appropriate weight matrix W that enables the FCM to accurately reproduce the historical response sequence of a dynamic system. Typically, weight learning methods can be categorized into three types: The first type is based on the Hebbian learning rule, which is a typical unsupervised learning algorithm [33]. It utilizes an iterative formula that relates the sequence samples and the given weights to the rate of change of the corresponding node values to iteratively adjust the weights of the FCM until a predetermined stopping criterion is met. This method relies more on a priori knowledge to design the FCM, and the values of its weight matrix are difficult to dynamically reflect the characteristics of changes in system data. The second type is based on swarm intelligence optimization learning methods, such as using Particle Swarm Optimization (PSO) [34] and Genetic Algorithms (GAs) [35]. The third type is a hybrid learning method, which combines the above two approaches [36].

In this study, we choose the least squares method to learn the weight matrix of FCMs rather than swarm-based learning algorithms (such as PSO or GA). This choice is primarily based on computational efficiency. The least squares method is relatively simple and efficient in computation, and it can quickly converge to the global optimal solution when dealing with large-scale data. For distribution grids, which have complex topological structures and a large number of nodes, swarm-based learning algorithms have a slower convergence speed and require more time, making it difficult to meet the needs of practical applications.

The topology of a distributed grid can be viewed as a network composed of edges and nodes [37], which is consistent with the topology of FCMs, and FCMs have good results in modeling complex systems. Thus, modeling the grid using FCMs by corresponding the nodes in the power system as nodes of FCMs is reasonable and effective. Figure 2 represents this process. First, the distribution grid node network is created by gathering the locations and connection relationships of substations, feeders, branch circuits, loads, and other power system elements and defining the topological links among the grid elements. Second, a FCM model with the same structure as the node network is developed based on the structure of the node network. Finally, the distribution grid's actual data is used as the values of the nodes, and the weight matrix of the fuzzy cognitive maps is trained to complete the distributed grid's FCM modeling. To acquire the time series of system voltage values $\boldsymbol{X}$, a distribution grid system with changeable loads is subjected to trend calculation based on node active and reactive power injection and repeated trend calculation utilizing Newton Raphson's approach in this study, where $\boldsymbol{X} = [\boldsymbol{X}_1, \boldsymbol{X}_2, ..., \boldsymbol{X}_n]$, $\boldsymbol{X}_j = \left[x_{1j}, x_{2j}, \ldots, x_{mj}\right]^T$, $j = 1, 2, \ldots, n$, n is the number of nodes in the

grid, and m is the length of the generated time series.

The elements in the column vector are normalized before learning the weight matrix to limit the influence of data discrepancies at different nodes of the distribution grid. The normalization formula is:

$$u^* = \frac{x - \min\left(\boldsymbol{X}_j\right)}{\max\left(\boldsymbol{X}_j\right) - \min\left(\boldsymbol{X}_j\right)} \tag{3.1}$$

where u is the normalized state value and $\boldsymbol{X}$ is the actual value. The normalized time series will be used later with the FCMs weight matrix learning. U can be stated as:

$$\boldsymbol{U} = \begin{bmatrix} u_{11} & u_{12} & \cdots & u_{1n} \\ u_{21} & u_{22} & \cdots & u_{2n} \\ \vdots & \vdots & & \vdots \\ u_{m1} & u_{m2} & \cdots & u_{mn} \end{bmatrix} \tag{3.2}$$

Taking $\boldsymbol{U}$ as the conceptual node value of the fuzzy cognitive maps, the vector form of Eq. (1) can be expressed as:

$$\boldsymbol{A}_j(t+1) = f(\boldsymbol{A}(t)W_j) \tag{3.3}$$

where $\boldsymbol{A}(t) = [\boldsymbol{A}_1(t), \boldsymbol{A}_2(t), \ldots, \boldsymbol{A}_n(t)]$ denotes the state value of n nodes at time t , $\boldsymbol{A}_j(t+1)$ is the state value of node j at time $t+1$, and $\boldsymbol{W}_j = \left[w_{1j}, w_{2j}, \ldots w_{nj},\right]^T$ is the jth column of the weight matrix $\boldsymbol{W}$.

The vectorized Eq. (7) can be expressed after inverse transformation as:

$$f^{-1}(\boldsymbol{A}_j(t+1)) = \boldsymbol{A}(t)\boldsymbol{W}_j \tag{3.4}$$

where f^{-1} is the sigmoid function following the inverse transformation. Eq. (8) is changed to generate a set of linear equations.

The time series obtained after normalization of the raw voltage data can be expressed as $\boldsymbol{U} = [\boldsymbol{U}_1, \boldsymbol{U}_2, \ldots, \boldsymbol{U}_m]^T$, $\boldsymbol{U}_j = [u_{j1}, u_{j2}, \ldots, u_{jn}]$, $j = 1, 2, \ldots, m$. Let $\boldsymbol{Z} = [\boldsymbol{U}_1, \boldsymbol{U}_2, \ldots, \boldsymbol{U}_{m-1}]^T$ and $\boldsymbol{Y}_j = f^{-1}\left(\left[u_{2j}, u_{3j}, \cdots, u_{mj}\right]^T\right)$. Substituting them into Eq. (8), we have :

$$\boldsymbol{Y}_j = \boldsymbol{Z}\boldsymbol{W}_j \tag{3.5}$$

where $\boldsymbol{Z}$ and $\boldsymbol{Y}_j$ are the independent and dependent variables of the historical data, and the weight matrix learning problem can be turned into a restricted least squares issue. The objective function can be expressed as follows:

$$\begin{aligned} \arg\min_{\boldsymbol{W}_i} : \left\|\boldsymbol{Z}\boldsymbol{W}_j - \boldsymbol{Y}_j\right\|_2 + \alpha\left\|\boldsymbol{W}_j\right\|_1 \\ \text{s.t.}\left\|\boldsymbol{W}_j\right\|_\infty \leq 1 \end{aligned} \tag{3.6}$$

where $\left\|\boldsymbol{Z}\boldsymbol{W}_j - \boldsymbol{Y}_j\right\|_2$ is the least squares error between the predicted and observed values and $\alpha\left\|\boldsymbol{W}_j\right\|_1$ is the penalty function to prevent overfitting. The value of the α set to 0.1. The constraint $\left\|\boldsymbol{W}_j\right\|_\infty \leq 1$ is derived from the definition of the weight matrix, and the values of all weight matrix elements must fall inside the interval $[-1, 1]$. In this study, we convert Eq. (10) to a convex optimization problem with linear constraints and use the method given in [38] to find the best weight matrix solution. Algorithm 1 describes the overall process of modeling the distribution grid using FCMs.

Algorithm 1 Learning of Weight Matrix

Input:

$\boldsymbol{X}_1, \boldsymbol{X}_2, \ldots, \boldsymbol{X}_n$:$\boldsymbol{X}_S(S = 1, 2, \ldots, n)$ is the initial data for training the weight matrix ; The length of each data is $k + 1$

α : Parameter values of regularization

λ : Parameter values of sigmoid function;

Output:

$\boldsymbol{W}$: a $n-$by$-n$ weight matrix;

$\boldsymbol{W} \leftarrow 0^{n \times n}$

Normalization of a multidimensional time series $\boldsymbol{X}$

$\boldsymbol{Z} \leftarrow [\boldsymbol{X}_1[1:k,1]; \boldsymbol{X}_2[1:k,1]; \cdots; \boldsymbol{X}_n[1:k,1]]$;

$\boldsymbol{Y} \leftarrow [\boldsymbol{X}_1[2:k+1,1]; \boldsymbol{X}_2[2:k+1,1]; \cdots; \boldsymbol{X}_n[2:k+1,1]]$;

$Y_j \leftarrow -\frac{1}{\lambda} ln\left(\frac{1}{Y[:,j]} - 1\right)$;

$j \leftarrow 1$

while $j \leq n$ **do**

  $variable \leftarrow \boldsymbol{w}_j$;

  $objection \leftarrow \min : \left\|\boldsymbol{Z}\boldsymbol{W}_j - \boldsymbol{Y}_j\right\|_2 + \alpha\left\|\boldsymbol{W}_j\right\|_1$

  $constraint \leftarrow \left\|\boldsymbol{W}_j\right\|_\infty \leq 1$

  $problem \leftarrow (variable, objection, constraint)$

  $\boldsymbol{w}_j \leftarrow$ Solving the problem based on the convex optimization solver

  $W[:, j] \leftarrow w_j$

  $j \leftarrow j + 1$

end while

3.2. Critical node identification

The weight matrix in a FCMs can represent the causal relationships between nodes in the system, which makes the fuzzy cognitive maps interpretable. The value of the weights in the weight matrix establishes the intensity of the causal relationship and reflects the relative relevance of the nodes to each other; thus, the weight matrix can be used to quantify the influence of the nodes on the system. In FCMs, nodes with greater weight values play an important part in shaping system behavior and can influence the overall model's operation. Therefore, the nodes corresponding to the parts of the weight matrix with relatively high weight values have a higher degree of influence on other nodes in the distribution grid.

To quantify the influence of nodes within a system, we introduce the concept of conceptual centrality. Conceptual centrality expresses the measure of how strong the direct connections are between a concept node C_i and other nodes in a FCM [27]. Figure 3 illustrates that depending on the direction of the directed edges, centrality can be calculated as either in-degree centrality or out-degree centrality. In-degree centrality represents the extent of influence that other nodes have on node C_i. When analyzing key nodes in a distribution network, we should focus on out-degree centrality, as it explains the extent of influence that node C_i in the distribution network has on other nodes. By calculating the out-degree centrality of all nodes, we can identify the node with the greatest influence

on other nodes in the distribution network.

To quantify the influence of a node within a system, the importance of a node I can be defined by the out-degree centrality of node C_i, expressed as follows:

$$I = \sum_{j=1}^{n} |w_{ij}| \tag{3.7}$$

where w_{ij} is the value of the degree of influence of node C_i and C_j in the weight matrix. A larger value of I indicates that the corresponding node has a greater degree of influence on the grid.

Figure 4 shows the process of modeling the distribution network using FCMs. The process can be summarized as follows:

Step 1: Repeated tidal current calculation is performed on the distribution grid in terms of active power and reactive power of the nodes of the distribution grid, the impedance between the nodes, and the connection between the nodes of the distribution grid to obtain the voltage data of the nodes of the distribution grid.

Step 2: The raw data for learning the FCMs is the time series obtained after normalizing the raw voltage data, and the weight matrix is solved using a convex optimization solver based on the interior point approach.

Step 3: The original distribution grid is analyzed based on the learned weight matrix to identify the critical nodes in the distribution grid.

(a) In-degree (b) Out-degree

Figure 3. Conceptual centrality.

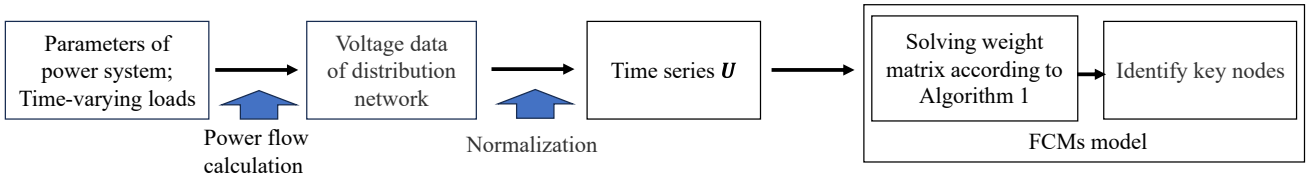

Figure 4. Distribution network modeling.

4. Case study

In this paper, repetitive power flow calculations are performed on distribution networks with time-varying loads to obtain voltage data for each node in the network, and FCMs are used to model the distribution network. Based on the topological structure of the distribution network, nodes in the distribution network, such as substations, distribution transformers, or customer loads, are treated as concept nodes in FCMs, while the connections between nodes represent power transmission lines. The actual operational data of the distribution network is then transformed into the input of node states for FCMs. The weight matrix of FCMs is learned from historical data to determine the causal relationship weights between nodes. By leveraging the semantic interpretability of FCMs, the out-degree centrality in the weight matrix is calculated to identify the key nodes that have the most significant impact on the performance of the distribution network. Finally, based on the results of the key node identification, strategies for the integration of distributed photovoltaic power are developed, and the voltage fluctuations and energy losses of the system before and after the integration of distributed photovoltaics with different penetration rates are compared, demonstrating the effectiveness and feasibility of the approach.

4.1. Evaluation metric

To calculate the degree of influence of each node in the distribution grid on the system based on the learned weight matrix, and to accurately evaluate the performance of the distribution grid operation, the following metrics are constructed.

4.1.1. Photovoltaic penetration

Photovoltaic penetration is defined as the ratio of the rated installed PV capacity to the peak load of the distribution grid [39], expressed as:

$$\%\text{Penetration} = \frac{P_{\text{PV}}^{\text{rated}}}{P_{\text{load}}^{\text{peak}}} \tag{4.1}$$

It should be noted that PV penetration characterizes the installed capacity level, whereas the actual PV output varies over time and is modeled separately using a normalized PV generation profile.

4.1.2. Voltage Fluctuation Index (VFI)

To study the impact of the access of distributed power sources on the distribution grid voltage, a voltage fluctuation index is assumed to express the fluctuation of the distribution grid voltage distribution over a period of time. The voltage fluctuation index of the distribution grid as a whole is the average of the sum of the voltage deviation rates of all nodes at all moments, and the impact of accessing distributed power sources at key nodes on the system is investigated by comparing the voltage fluctuations under different accesses of distributed power sources. This can be expressed as follows:

$$VFI = \frac{\sum_{i=1}^{n}\sum_{t=1}^{T}|V_i(t) - V_0|}{nTV_0} \times 100\% \tag{4.2}$$

where VFI is the voltage fluctuation index, $V_i(t)$ is the actual voltage value of the system node i at time t , T is the length of time, n is the total number of nodes in the distribution grid, and V_0 is the standard voltage of the distribution grid. The smaller value of the voltage fluctuation index indicates that the voltage profile of the system is more stable after accessing the distributed power supply.

4.1.3. Power loss index

In the distribution grid system, the power loss of the system is analyzed by trend calculation, and the Total Power Loss(TPL) can be expressed as the following expression:

$$TPL = \sum_{t=1}^{T} \sum_{j=1}^{N} I_j^2(t) \times R_n \tag{4.3}$$

where T is the length of time, N is the number of branches in the system, and $I_j(t)$ denotes the magnitude of the current in branch j in the system at moment t. The value of the current can be obtained from the solution of the tidal current analysis, and R_j represents the resistance of branch j.

To measure the degree of reduction of power losses in the distribution grid after accessing distributed PV, the power loss index can be expressed as:

$$E_{loss} = \frac{TPL_0 - TPL_{PV}}{TPL_0} \times 100\% \tag{4.4}$$

where TPL denotes the value of electrical energy loss in the absence of PV access, and TPL_{PV} indicates the value of electrical energy loss in case of PV access. From Eq. (15), the larger value of E_{loss} indicates that the degree of reduction of losses in the distribution grid after PV access will be higher, and the better the effect of PV access will be.

4.2. Load and PV modeling

In this research, modeling the distributed grid parameters with FCMs necessitates time-varying load models. The typical load curves shown in Figure 5 are selected from real measured load data and are applied to the 33-node and 118-node test systems, where they are randomly assigned to different nodes to represent load variability.

As shown in Figure 6, a normalized PV generation profile is adopted in this study [40]. While different PV penetration levels correspond to different installed PV capacities, the temporal variation of PV output is assumed to follow the same per-unit curve, and the actual PV power is calculated by multiplying the normalized values by the rated PV capacity at each penetration level.

4.3. Case 1:33-bus system

4.3.1. Case description

There are 33 nodes and 32 branches in the 33-bus system, where bus 1 is the external power node. The system structure diagram is shown in Figure 7 [41]. The maximum total load of the system used in the case is 3053 kW + 1460 kVA, and the first voltage of the system network is 12.66 kV. The load profile of the system over 24 h is shown in Figure 8. The system has a peak demand of 3053.7 kW in

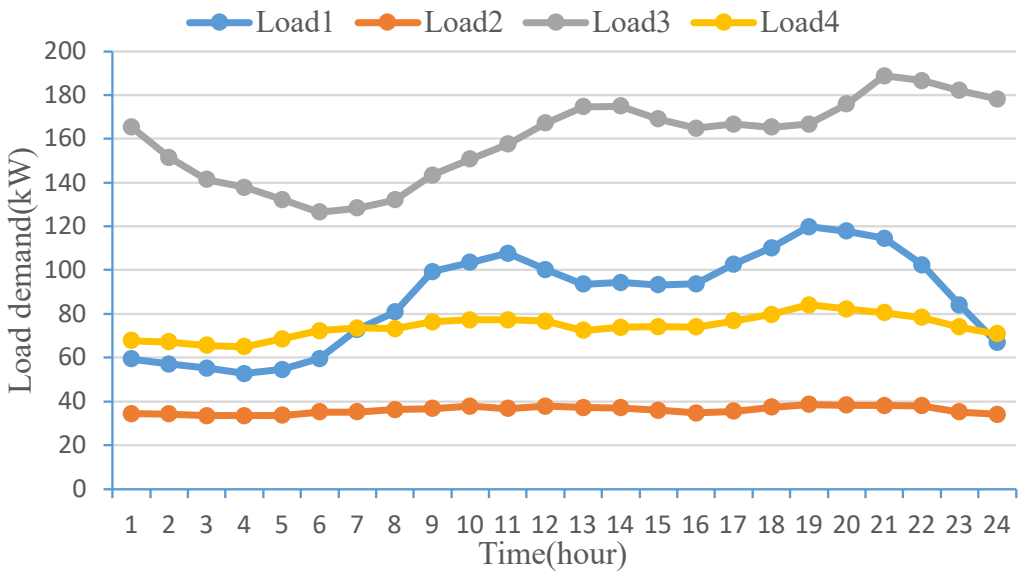

Figure 5. Typical daily load curve.

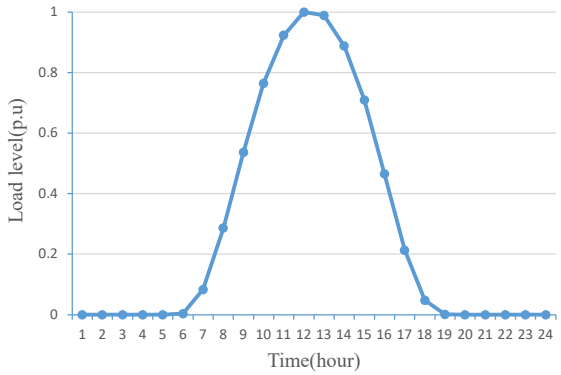

Figure 6. PV daily output curve.

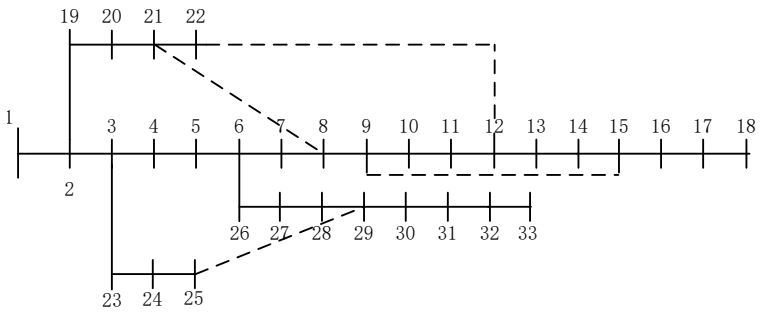

Figure 7. 33-bus system.

the load profile and a trough load of 2214.1 kW. The 24 h voltage distribution of the system without any PV is shown in Figure 9.

In this case, the peak loss of the system occurs at hour 21 as 141.3 kW, and the minimum loss is 73.0 kW at hour 4.

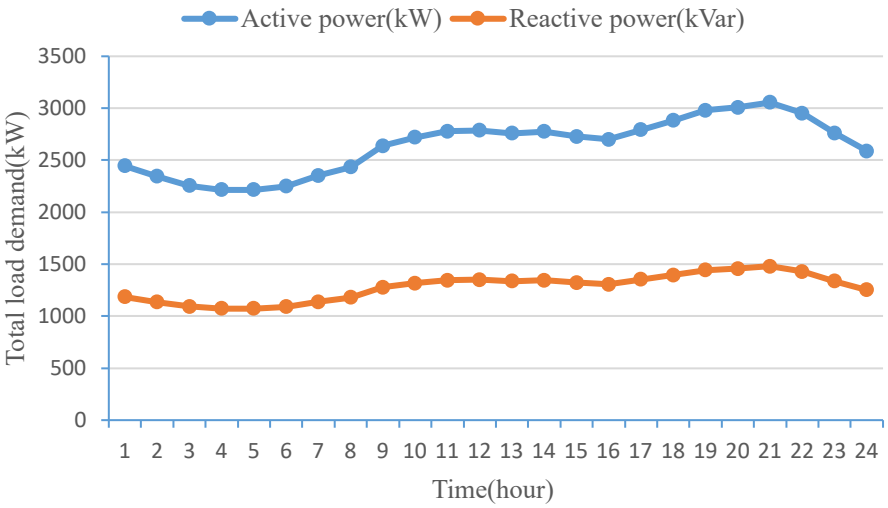

Figure 8. System 24 h total load curve.

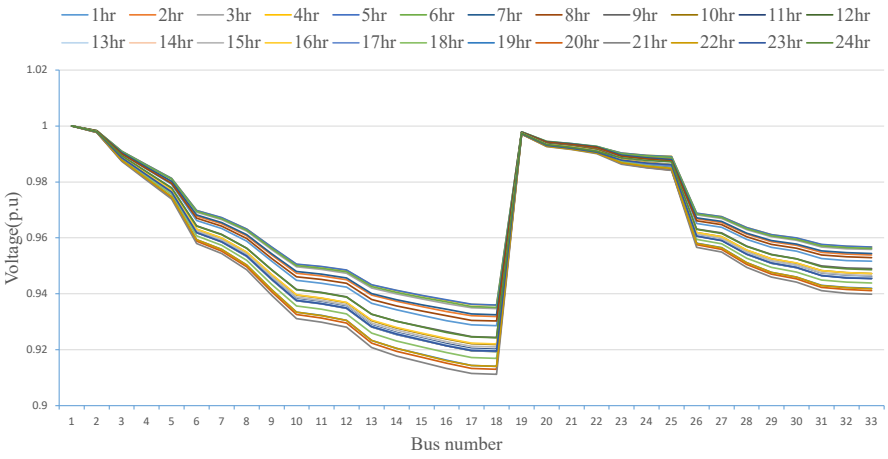

Figure 9. Voltage without PV for 33 bus system.

4.3.2. Critical node identification results and analysis

The influence metrics are calculated by learning the weight matrix of the FCMs, and the nodes with higher influence metrics have a higher degree of influence in the grid. Therefore, access to distributed power sources at these nodes should be avoided to maintain the stability of the system voltage. The results of the nodal importance calculation for the distribution grid are shown in Figure 10. The results of the top 10 nodes in terms of node impact ranking are shown in Table 2. According to the results in Table 2, the distributed access strategy is selected, the impact of different access strategies on the

distribution grid is compared, and the distribution grid is studied according to the two ways of critical node access and non-critical node access, respectively. The indicators of the distribution grid are calculated under different penetration rates.

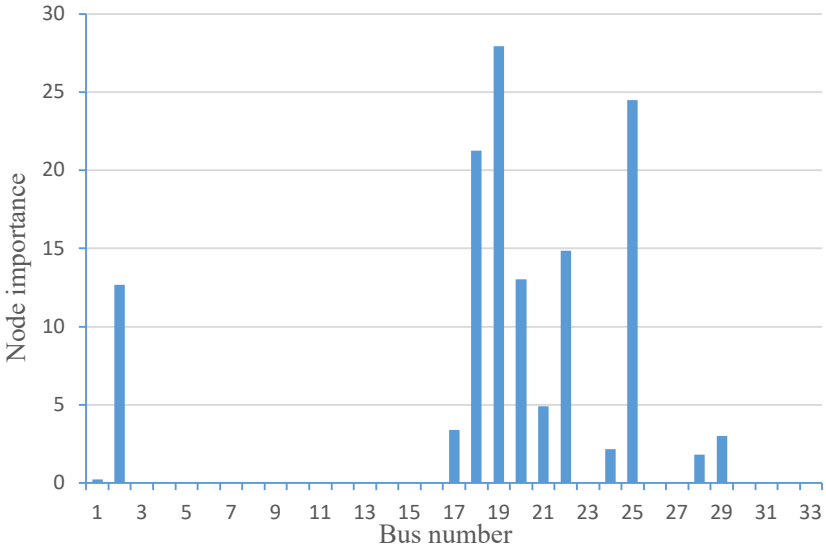

Figure 10. Node Importance of 33 bus system.

Table 2. Importance results of 33 bus system.

Importance ranking	Node number	Node Importance
1	19	27.9412
2	25	24.4944
3	18	21.2698
4	22	14.8447
5	20	13.0183
6	2	12.6885
7	21	4.9181
8	17	3.3985
9	29	3.0037
10	24	2.1864

In the case studies, PV systems are assumed to be connected to 30% of the network nodes, and the nodes with the lowest 30% importance index values are selected as candidate PV access locations. Table 3 summarizes the results of the distribution grid metrics at different penetration rates and with different access methods. Table 3 shows that as PV is connected to the distribution grid with different penetration rates, when the PV penetration rate increases, the voltage fluctuations and power losses of the system are reduced to a certain extent, regardless of the way distributed PV is connected. However, when PV penetration continues to increase, voltage fluctuations instead increase due to voltage boosting by distributed PV, and voltage overrun problems may occur. On the other hand, for the same PV penetration rate, the voltage fluctuation and energy loss of the system with distributed PV accessed by critical nodes are greater than the system with distributed PV accessed by non-critical

nodes, according to the comparison of experimental results.

Table 3. Distribution grid indices at different penetration rates for 24 h.

PV penetration(%)	Connected model	VFI(%)	E_{loss}(%)
0	None	3.8585	None
20	Crit.	3.5872	15.2336
	Non-Crit.	3.3594	28.5089
40	Crit.	3.3298	27.8622
	Non-Crit.	3.3594	37.5295
60	Crit.	3.0597	35.2463
	Non-Crit.	2.6656	45.5577
80	Crit.	2.8710	35.6776
	Non-Crit.	2.7098	41.8918

Crit:Connected by critical nodes.
Non-Crit:Connected by non-critical nodes.

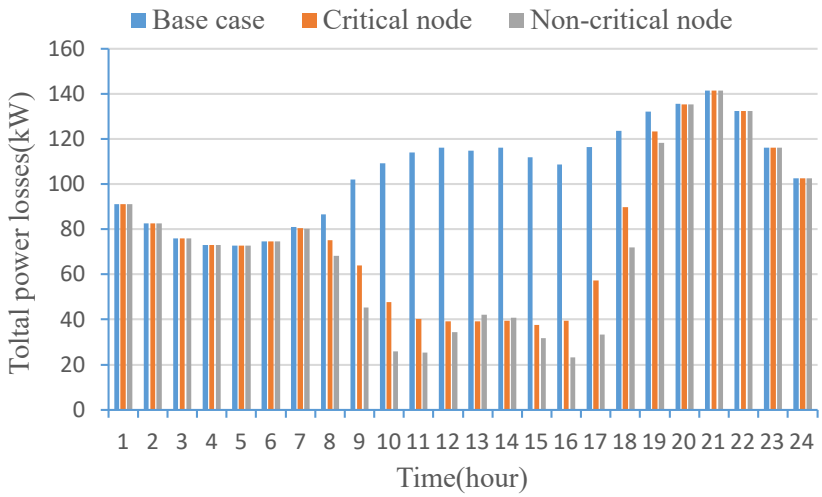

Figure 11. Energy loss under different access methods for 24 h.

Figure 11 shows the hourly energy loss of the system for both access methods over a 24 h period for a penetration rate of 60%. When the PV output starts to increase, the energy loss under the two access methods starts to decrease, but the energy loss of the non-critical node access method is slightly higher than that connected with critical node in the 13th and 14th hours, and the energy loss is equal to or less than that connected with critical node in all other cases. During the 24 hours, the power loss in the distribution grid under the standard system is 2530.13 kW, the total loss under connected with critical node is 1870.73 kW, and the total loss under that connected with non-critical node is 1738.21 kW. Therefore, being connected with a non-critical node is more effective in reducing losses in the distribution system.

Figure 12 shows a comparison of the distribution grid node voltage curves when the PV output power reaches its maximum value (hour 13) at 30% PV penetration. In the standard case, the lowest point of voltage occurs at bus 18 (0.918p.u). In the case of PV access to the critical node, the lowest

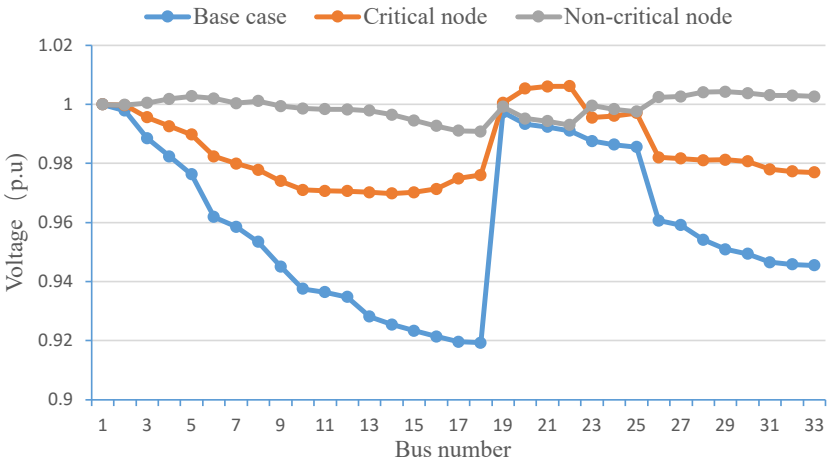

Figure 12. Distribution grid node voltage at hour 13.

voltage point occurs at bus 14 (0.969 p.u), and the highest voltage point is at bus 22 (1.006 p.u). The voltages in the system have been increased somewhat except for bus 1 and bus 19. In the case of PV access to the non-critical node, the lowest point of voltage occurs at bus 18 (0.991p.u), and the highest point of voltage occurs at n bus 29 (1.004p.u). The voltage volatility is 0.12%, which is 3.95% lower compared to the volatility of 4.07% in the base case. In summary, although either way of access has a certain effect on the distribution grid voltage enhancement, compared to accessing in a critical node way, accessing in a non-critical node way makes the distribution grid voltage trend smoother, and the highest and lowest point voltages are better than accessing PV in a critical node way.

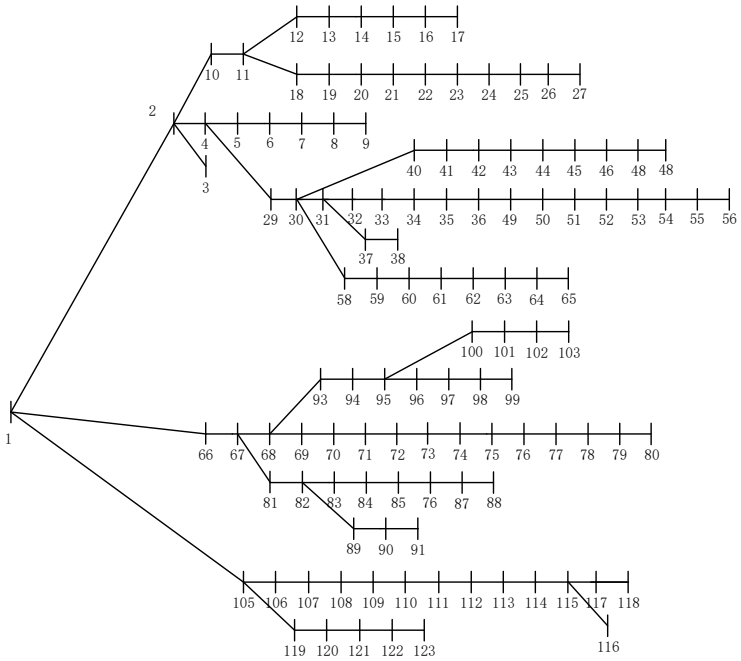

Figure 13. 118 bus system.

4.4. Case2:118 bus system

4.4.1. Case description

The test system is a distributed system containing 118 nodes, and the distribution grid structure is shown in Figure 13, where node 1 is an external power node and the rest of the load nodes are PQ nodes; the original network structure and line parameters are visible [42]. The system peak load demand is set to 21777.8 kW and 10547.4kvar, and the standard system voltage is 11 kV.

The 24 h voltage variation of the system without PV connection is shown in Figure 14. At this time, the daily power loss of the system is 13533 kW and the voltage fluctuation index of the system is 3.04%.

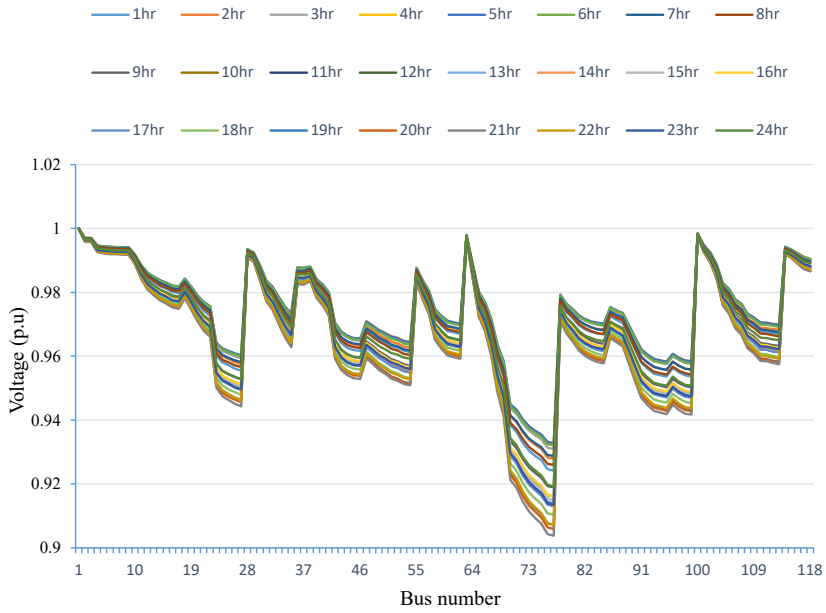

Figure 14. Voltage without PV for 118 bus system.

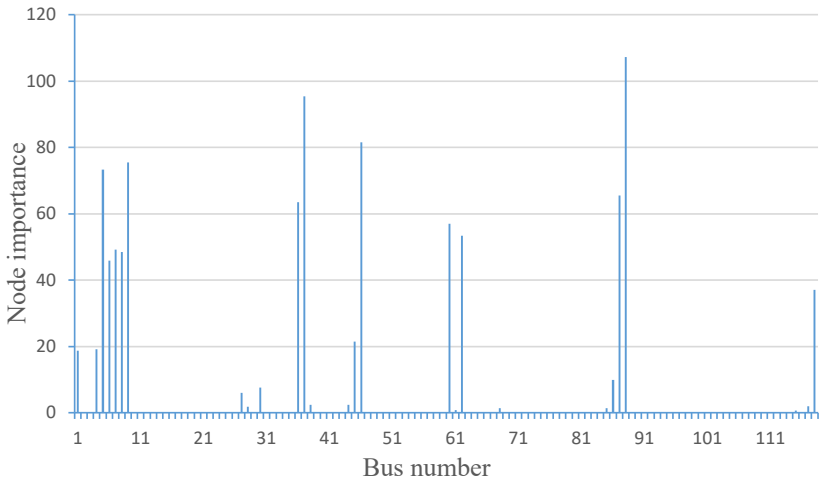

Figure 15. Node Importance of 118 bus system.

4.4.2. Time series key node identification results and analysis

Based on the results of the trend calculation, key nodes are identified for the 118-node distribution system. The top ten nodes in terms of node importance and their corresponding importance index values are given in Table 4, and the results of the node importance calculation are shown in Figure 15. To verify the effectiveness of key node identification, distributed PV with different penetration rates are accessed to the distribution grid, and relevant indicators are calculated. Moreover, considering the high number of nodes in the 118-node system, 30% of all nodes are selected to access distributed PV. Table 5 shows the results of calculation of individual indicators according to PV penetration rates.

Table 4. Importance results of 118 bus system.

Importance ranking	Node number	Node Importance
1	88	107.2394
2	37	95.3590
3	46	81.5160
4	9	75.4543
5	5	73.3703
6	87	65.5849
7	36	57.0007
8	60	53.3835
9	62	49.1698
10	7	48.4927

Table 5. Distribution grid indices at different penetration rates for 24 h.

PV penetration(%)	Connected model	VFI(%)	E_{loss}(%)
0	None	3.0435	—
20	Crit.	2.8827	10.72
	Non-Crit.	2.7621	20.93
40	Crit.	2.7247	17.16
	Non-Crit.	2.4859	37.74
60	Crit.	2.6322	17.93
	Non-Crit.	2.2290	44.56
80	Crit.	2.5878	13.15
	Non-Crit.	2.1169	38.99

The PV penetration of 60% shown in Figure 16 is the value of the system voltage at node 118 when PV output is at its maximum (hour 13). Regardless of the way PV is connected, the voltage at all nodes is increased compared to the original distribution system. However, the voltage fluctuations after accessing PV at critical nodes are significantly greater than accessing at non-critical nodes, and exceeding the standard distribution grid node voltages occurs at some nodes of the distribution grid voltage.

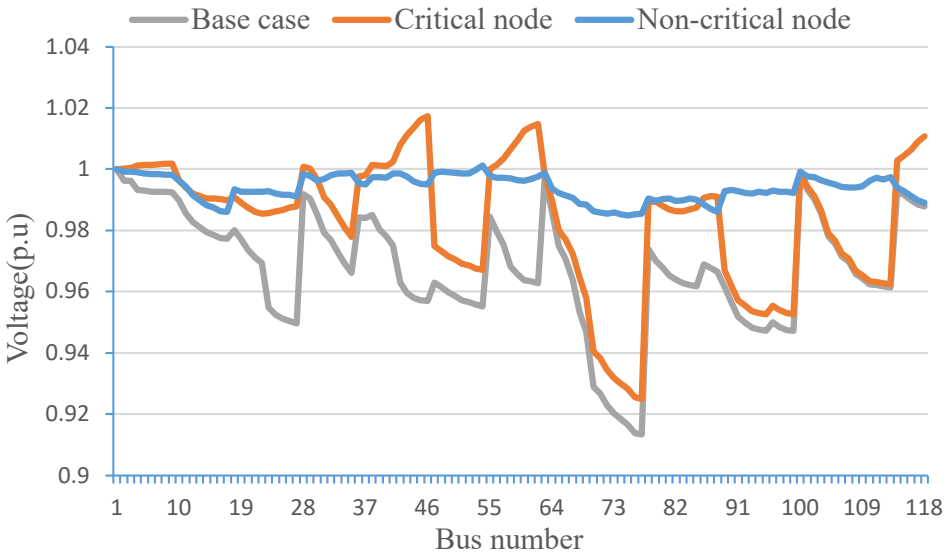

Figure 16. Distribution grid node voltage at hour 13.

4.5. Comparison of methods

The results are compared with those obtained using the Local Particle Swarm Optimization Variant (LPSOV) [43], Load Shock Vulnerability [44], and PageRank [45]. All comparative experiments are conducted on the IEEE 33-bus model under a 60% photovoltaic penetration level, deploy distributed photovoltaic systems at non-critical nodes, and both voltage fluctuation and power-loss indices after distributed-PV integration are calculated. The outcomes are presented in Table 6.

Table 6. Identification and sort based on different methods.

Method	VFI(%)	$E_{loss}(\%)$
LPSOV	2.7390	38.3926
Load Shock Vulnerability	3.3659	17.9594
PageRank	2.6627	44.7162
Method in this paper	2.6656	45.5577

Table 6 summarizes the performance of different node identification methods in terms of the voltage fluctuation index (VFI) and the energy loss improvement index $E_{loss}(\%)$. As shown in the table, the VFI values obtained by the different methods are within a relatively close range. The method proposed in this paper yields a VFI of 2.6656, which is comparable to the results obtained by the PageRank method (2.6627) and lower than those of the LPSOV and Load Shock Vulnerability methods. This indicates that similar levels of voltage fluctuation control are achieved among several methods under the same simulation conditions.

With respect to the energy loss indicator, noticeable differences can be observed among the methods. The proposed method results in an $E_{loss}(\%)$ value of 45.5577%, which is higher than the values obtained by the other comparison methods. The PageRank method also shows a relatively high $E_{loss}(\%)$, while the Load Shock Vulnerability method exhibits a much lower value. These results suggest that different node identification strategies may lead to different impacts on system energy loss

characteristics, even when their voltage fluctuation performance is comparable. In this comparison, a lower VFI indicates better voltage stability, while a higher $E_{loss}(\%)$ represents a larger reduction in system energy losses after PV integration.

Overall, the comparison indicates that the proposed method provides a combination of relatively low voltage fluctuation and high energy loss reduction under the tested conditions, offering a distinct performance profile compared with the other methods considered.

5. Conclusions

In this paper, we presents a method based on FCMs to determine the connection points of PV systems in distribution networks, addressing the issues of significant voltage fluctuations and high energy losses that arise after the integration of distributed PV into the distribution network. The method employs load characteristics with time-varying properties and typical distributed PV outputs to simulate the distribution network. Subsequently, it transforms the solution of the FCM weight matrix into a least squares problem, forming a novel approach to modeling the distribution network. It then utilizes the out-degree centrality of nodes to identify the connection points for distributed PV systems. Finally, the method is validated in the IEEE standard node distribution system. The experimental results demonstrate that the interpretability of FCMs is effective in identifying key nodes in the distribution network. When selecting connection points, it is advisable to choose non-critical nodes for the integration of distributed PV, which can significantly improve the voltage distribution of the distribution network and reduce network losses.

The study on the identification of key nodes for distributed PV based on FCMs can serve as a starting point for further research. We hope to establish multi-layer FCMs using data attributes (such as voltage, current, power, and phase angle) for modeling distribution networks. Moreover, with the widespread application of distributed PV systems, research on the collaborative optimization of FCMs in photovoltaic and energy storage systems, electric vehicles, and other distributed resources will also become a research focus.

Author contributions

Jiancheng Sha: Software, Investigation, Validation, Writing-original draft; Shaojun Bian: Conceptualization, Investigation, Methodology, Validation; Lingfang Sun: Project administration, Formal analysis, Supervision; Mengchao Xu: Formal analysis; Guoliang Feng: Investigation, Formal analysis. All authors have read and approved the final version of the manuscript for publication.

Use of Generative-AI tools declaration

The authors declare they have not used Artificial Intelligence (AI) tools in the creation of this article.

Acknowledgments

This research was financially supported by the National Natural Science Foundation of China [Grant No.52376096].

Conflict of interest

The authors declare no conflicts of interest in this paper.

References

1. Khalil AE, Sedky JS, Ibrahim AM, Boghdady TA (2025) Optimal placement and sizing of distributed energy resources in active distribution networks under uncertainty: A multi-objective approach using electric eel foraging optimization. *Comput Electr Eng* 128: 110715. https://doi.org/10.1016/j. compeleceng.2025.110715
2. Adegoke SA, Sun Y, Adegoke AS, Ojeniyi D (2024) Optimal placement of distributed generation to minimize power loss and improve voltage stability. *Heliyon* 10(21): e39298. https://doi.org/10.1016/j.heliyon.2024.e39298
3. Liu B, Li Z, Chen X, Huang Y, Liu X (2018) Recognition and vulnerability analysis of key nodes in power grid based on complex network centrality. *IEEE Transactions on Circuits and Systems II: Express Briefs* 65: 346–350. https://doi.org/10.1109/TCSII.2017.2705482
4. Zhu D, Wang H, Wang R, Duan J, Bai J (2018) Identification of key nodes in a power grid based on modified PageRank algorithm. *Energies* 15: 797. https://doi.org/10.3390/en15030797
5. Liu M , Zhao L , Huang L, Zhang X, Deng C, Long Z (2017) Identification of Critical Lines in Power System Based on Optimal Load Shedding. *Energy and Power Engineering* 9: 261–269. https://doi.org/10.4236/epe.2017.94b031
6. Yang L, Li C, Ma J, Liu S (2022) Research on Identification Model of Weak Area of New Energy Grid Considering Operation Risk and Transient Stability Constraints. *2022 Power System and Green Energy Conference (PSGEC)* 2022: 1190–1194. https://doi.org/10.1109/PSGEC54663.2022.9881053
7. Zhang W, Liu KY, Sheng W, Du S, Jia D (2022) Critical node identification in active distribution network using resilience and risk theory. *IET Gener Transm Dis* 14: 2771–2778. https://doi.org/10.1049/iet-gtd.2019.1781
8. Wang J, Gu X, Wang T, Zhang S (2017) Power system critical node identification based on power tracing and link analysis method. *Power System Protection and Control* 45: 22–29. https://doi.org/10.7667/PSPC160434
9. Liu Z, Sheng W, Su J, Du S, Xia Y, Wang J (2022) Dynamic identification of key nodes in active distribution network for operation optimisation requirements. *IET Gener Transm Dist* 17: 1081–1096. https://doi.org/10.1049/gtd2.12682
10. Feng G, Zhang L, Yang J, Lu W (2021) Long-term prediction of time series using fuzzy cognitive maps. *Eng Appl Artif Intel* 102: 104274. https://doi.org/10.1016/j.engappai.2021.104274
11. Yue W, Chen X, Huang K, Zeng Z, Xie Y (2018) Knowledge modeling for root cause analysis of complex systems based on dynamic fuzzy cognitive maps. *IFAC-PapersOnLine* 51: 13–18. https://doi.org/10.1016/j.ifacol.2018.09.385

12. Obiedat M, Samarasinghe S (2018) A novel semi-quantitative Fuzzy Cognitive Map model for complex systems for addressing challenging participatory real life problems. *Appl Soft Comput* 48: 91–110. https://doi.org/10.1016/j.asoc.2016.06.001

13. Feng G, Lu W, Yang J (2022) Modeling time series using multi-modality fuzzy cognitive maps. *Journal of System Simulation* 34: 543–554. https://doi.org/10.16182/j.issn1004731x.joss.20-0834

14. Li S, Wang J, Zhang H, Liang Y (2024) Enhancing hourly electricity forecasting using fuzzy cognitive maps with sample entropy. *Energy* 298: 131429. https://doi.org/10.1016/j.energy.2024.131429

15. Qin D, Peng Z, Wu L (2023) Deep attention fuzzy cognitive maps for interpretable multivariate time series prediction. *Knowledge-Based Systems* 275: 110700. https://doi.org/10.1016/j.knosys.2023.110700

16. Bakhtavar E, Valipour M, Yousefi S, Sadiq R, Hewage K (2021) Fuzzy cognitive maps in systems risk analysis: a comprehensive review. *Complex Intell Syst* 7: 621–637. https://doi.org/10.1007/s40747-020-00228-2

17. Azar A, Dolatabad KM (2019) A method for modelling operational risk with fuzzy cognitive maps and Bayesian belief networks. *Expert Syst Appl* 115: 607–617. https://doi.org/10.1016/j.eswa.2018.08.043

18. Salmeron JL, Lopez C (2011) Forecasting risk impact on ERP maintenance with augmented fuzzy cognitive maps. *IEEE T Software Eng* 38: 439–452. https://doi.org/10.1109/TSE.2011.8

19. Szwed P (2021) Classification and feature transformation with fuzzy cognitive maps. *Appl Soft Comput* 105: 107271. https://doi.org/10.1016/j.asoc.2021.107271

20. Song HJ, Miao CY, Wuyts R, Shen ZQ, D'Hondt M, Catthoor F (2010) An extension to fuzzy cognitive maps for classification and prediction. *IEEE T Fuzzy Syst* 19: 116–135. https://doi.org/10.1109/TFUZZ.2010.2087383

21. Hilal AM, Alsolai H, Al-Wesabi FN, Nour MK, Motwakel A, Kumar A, et al. (2022) Fuzzy Cognitive Maps with Bird Swarm Intelligence Optimization-Based Remote Sensing Image Classification. *Comput Intel Neurosc* 2022: 4063354. https://doi.org/10.1155/2022/4063354

22. Tyrovolas M, Liang XS, Stylios C (2022) Information flow-based fuzzy cognitive maps with enhanced interpretability. *Granular Comput* 8: 2021–2038. https://doi.org/10.1007/s41066-023-00417-7

23. Papageorgiou EI, Salmeron JL (2012) A review of fuzzy cognitive maps research during the last decade. *IEEE T Fuzzy Syst* 21: 66–79. https://doi.org/10.1109/TFUZZ.2012.2201727

24. Liu X, Wang Z, Zhang S, Liu J (2019) A novel approach to fuzzy cognitive map based on hesitant fuzzy sets for modeling risk impact on electric power system. *Int J Comput Intel Syst* 12: 842–854. https://doi.org/10.2991/ijcis.d.190722.001

25. Kyriakarakos G, Dounis AI, Arvanitis KG, Papadakis G (2012) A fuzzy cognitive maps–petri nets energy management system for autonomous polygeneration microgrids. *Appl Soft Comput* 12: 3785–3797. https://doi.org/10.1016/j.asoc.2012.01.024

26. Karagiannis IE, Groumpos PP (2013) Modeling and analysis of a hybrid-energy system using fuzzy cognitive maps. *21st Mediterranean Conference on Control and Automation*, 257–264. https://doi.org/10.1109/MED.2013.6608731
27. Kosko B (1986) Fuzzy cognitive maps. *International journal of man-machine studies* 24: 65–75. https://doi.org/10.1016/S0020-7373(86)80040-2
28. Tsadiras AK (2008) Comparing the inference capabilities of binary, trivalent and sigmoid fuzzy cognitive maps. *Inform Sciences* 178: 3880–3894. https://doi.org/10.1016/j.ins.2008.05.015
29. Nápoles G, Papageorgiou E, Bello R, Vanhoof K (2016) On the convergence of sigmoid fuzzy cognitive maps. *Inform Sciences* 349: 154–171. https://doi.org/10.1016/j.ins.2016.02.040
30. Yang Z, Liu J (2020) Learning fuzzy cognitive maps with convergence using a multi-agent genetic algorithm. *Soft Computing* 24: 4055–4066. https://doi.org/10.1007/s00500-019-04173-2
31. Nápoles G, Concepción L, Falcon R, Bello R, Vanhoof K (2017) On the accuracy–convergence tradeoff in sigmoid fuzzy cognitive maps. *IEEE T Fuzzy Syst* 26: 2479–2484. https://doi.org/10.1109/TFUZZ.2017.2768327
32. Bueno S, Salmeron JL (2009) Benchmarking main activation functions in fuzzy cognitive maps. *Expert Syst Appl* 36: 5221–5229. https://doi.org/10.1016/j.eswa.2008.06.072
33. Papakostas GA, Koulouriotis DE, Polydoros AS, Tourassis VD (2012) Towards Hebbian learning of fuzzy cognitive maps in pattern classification problems. *Expert Syst Appl* 39: 10620–10629. https://doi.org/10.1016/j.eswa.2012.02.148
34. Liang W, Zhang Y, Liu X, Wang J, Yang Y (2022) Towards improved multifactorial particle swarm optimization learning of fuzzy cognitive maps: a case study on air quality prediction. *Appl Soft Comput* 130: 109708. https://doi.org/10.1016/j.asoc.2022.109708
35. Altundogan TG, Karakose M (2020) Genetic algorithm based fuzzy cognitive map concept relationship determination and sigmoid configuration. *2020 IEEE International Symposium on Systems Engineering (ISSE)* 2020: 1–5. https://doi.org/10.1109/ISSE49799.2020.9272216
36. Rezaee MJ, Yousefi S, Babaei M (2017) Multi-stage cognitive map for failures assessment of production processes: an extension in structure and algorithm. *Neurocomputing* 232: 69–82. https://doi.org/10.1016/j.neucom.2016.10.069
37. Wen J, Tan Y, Jiang L, Lei K (2018) Dynamic reconfiguration of distribution networks considering the real-time topology variation. *IET Gener Transm Dis* 12: 1509–1517. https://doi.org/10.1049/iet-gtd.2017.1304
38. Lu W, Feng G, Liu X, Pedrycz W, Zhang L, Yang J (2018) Fast and effective learning for fuzzy cognitive maps: A method based on solving constrained convex optimization problems. *IEEE T Fuzzy Syst* 28: 2958–2971. https://doi.org/10.1109/TFUZZ.2019.2946119
39. Cheng D, Mather BA, Seguin R, Hambrick J, Broadwater RP (2015) Photovoltaic (PV) impact assessment for very high penetration levels. *IEEE J Photovolt* 6: 295–300. https://doi.org/10.1109/JPHOTOV.2015.2481605
40. Zhuo Z, Zhang N, Yang J, Kang C, Smith C, O'Malley MJ, et al. (2019) Transmission expansion planning test system for AC/DC hybrid grid with high variable renewable energy penetration. *IEEE T Power Syst* 35: 2597–2608. https://doi.org/10.1109/TPWRS.2019.2959508

41. Gilani MA, Kazemi A, Ghasemi M (2020) Distribution system resilience enhancement by microgrid formation considering distributed energy resources. *Energy* 191: 116442. https://doi.org/10.1016/j.energy.2019.116442

42. Zhang D, Fu Z, Zhang L (2007) An improved TS algorithm for loss-minimum reconfiguration in large-scale distribution systems. *Electr Power Syst Res* 77: 685–694. https://doi.org/10.1016/j.epsr.2006.06.005

43. Gkaidatzis PA, Bouhouras AS, Doukas DI, Sgouras KI, Labridis DP (2017) Load variations impact on optimal DG placement problem concerning energy loss reduction. *Electr Power Syst Res* 152: 36–47. https://doi.org/10.1016/j.epsr.2017.06.016

44. Ding M, Han P (2007) An improved TS algorithm for loss-minimum reconfiguration in large-scale distribution systems. *Proceedings-Chinese Society of Electrical Engineering* 28: 20. https://doi.org/10.13334/j.0258-8013.pcsee.2008.10.004

45. Zhu D, Wang R, Cheng W, Duan J, Wang H (2022) Critical transmission node identification method based on improved PageRank algorithm. *Power System Protection and Control* 50: 86–93. https://doi.org/10.19783/j.cnki.pspc.210567

AIMS Press